Experimental investigation and phase shift analysis of low-energy electron-helium scattering

J. Phys. B: Atom. Molec. Phys., Vol. 8, No. 3, 1975. Printed in Great Britain.

Experimental investigation and phase shift analysis of low-energy electron–helium scattering

D Andrick and A Bitsch

Fachbereich Physik, University Trier-Kaiserslautern, West Germany

Received 8 July 1974

Abstract. The angular distribution of electrons scattered elastically from helium atoms has been measured in the energy range from 2 to 19 eV. The experimental data have been fitted by the partial wave formula to determine the scattering phase shifts. From these, absolute values of the differential and the total cross sections were computed. The accuracy of the measured shape of the angular distributions is better than 5%, of the absolute calibration between 20% at low and 5% at high energies. The discrepancy between earlier experiments and theoretical predictions is removed in favour of theory.

1. Introduction

The scattering of low-energy electrons from atoms has been investigated since the early thirties (for a summary see Massey and Burhop 1969). Predominantly the rare gases, and among these most frequently helium, have been studied experimentally several times by various methods. The results obtained for the differential (Ramsauer and Kollath 1932, Bullard and Massey 1931, Mehr 1967, Gibson and Dolder 1969a), total (eg Ramsauer 1921, Normand 1930, Ramsauer and Kollath 1932, Golden and Bandel 1964; for a critical comparison see Bederson and Kieffer 1971) and momentum transfer cross sections (Frost and Phelps 1964, Crompton *et al* 1970) show only qualitative agreement between each other, and are not consistent with modern theoretical work (eg Duxler *et al* 1971), so that a simultaneous analysis of those experiments fitting best together (Bransden and McDowell 1969, McDowell 1971) yields scattering phase shifts in poor agreement with computed values.

The latter fact leads to the situation that up to now no theoretical approach can be ruled out from experimental facts.

On the experimental side, for differential cross section measurements in which high-energy resolution is required, it is especially difficult to attain a calculable scattering geometry together with a sufficiently narrow and well-shaped instrumental energy distribution profile. So concentration may be placed upon the energy resolution performance only and the efficiency as a function of the scattering angle may then be determined by comparison of a measured angular distribution with a known one. Thus there is often a need for a well-known differential cross section to calibrate an apparatus.

Presently no reliable differential cross section is established in low-energy electron scattering at all which may be trusted to be accurate to 10 per cent or better. Therefore it seemed worthwhile to remeasure the differential cross section of the elastic electron–helium scattering once more, and to try to clear up the discrepancies.

2. Experimental apparatus and procedure

In most cases (eg Ramsauer and Kollath 1932, Gibson and Dolder 1969a) differential cross sections have been measured using a scattering chamber, so that a correction had to be made to take account for the change of the scattering volume with angle (eg Chamberlain *et al* 1970). The determination of this correction is not simple especially in low-energy work (Andrick 1973). To avoid this difficulty we have used a cross beam technique which does not require a correction to the original data and does not make as heavy demands on the focusing of the electron beam.

A diagram of the apparatus is given in figure 1. The electron gun produces an energy-selected beam of 50 meV energetic width and a current of about 10^{-7} A. This is crossed with a target gas beam having a peak pressure of about 10^{-3} Torr. The scattered electrons traverse two cylindrical electrostatic analysers in the detector and are counted by a multiplier. The scattering angle can be varied by sweeping the electron gun. On the one side of the zero direction a maximum angle of 145° and on the other side 100° can be achieved.

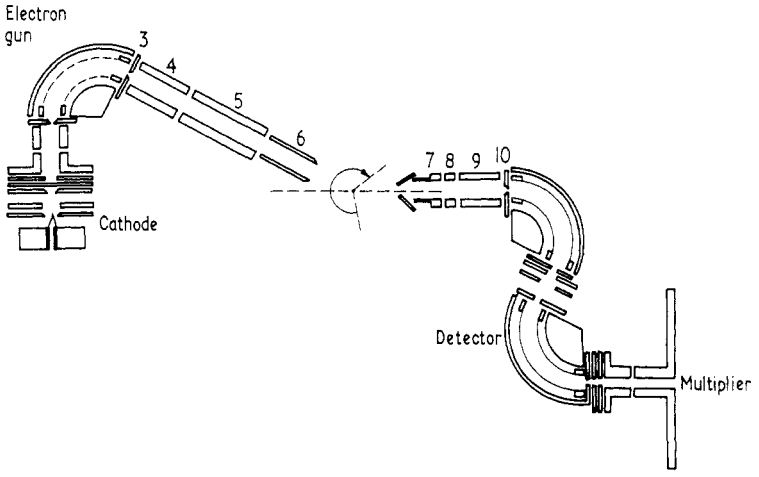

Figure 1. Diagram of the apparatus.

2.1. Electron gun

The electrons emitted by a tungsten filament are focused by a lens system to the entrance aperture of a cylindrical electrostatic analyser. The energy spectrum is expanded on the output aperture and a certain fraction of the energy band can pass the exit slit. Entrance and output slits have widths of 0·3 mm, the main radius of the analyser is 17·5 mm, and the mean energy of the electrons is about 3 eV.

In the lenses 4–6 the electrons are accelerated or slowed down to the energy desired in the collision, and are focused to the scattering centre.

2.2. Target beam source

The principle of the gas beam source is simple. The beam is generated by a tube of 0·4 mm inner diameter and has approximately a cosine distribution, as the pressure at the end of the tube is about 0·5 Torr. To cut off the wings of this distribution, a skimmer of 0·4 mm

diameter is placed at a distance of about 1 mm from the outlet of the tube. In this way a total width of the beam of about 2 mm is achieved in the plane of the electron beam about 2 mm beyond the skimmer. The beam profile was measured using a small ionization gauge head which was closed by a cap with a 0·2 mm hole.

It was found to be necessary to sharpen the edges of the skimmer and the top of the tube to reduce the number of target gas atoms scattered from these edges towards the scattering plane, thus causing wings to the beam profile.

We did not use a differential pumping system and the atoms intercepted by the skimmer caused the main contribution to the background pressure. This was about 10^{-4} Torr helium in the whole apparatus, whereas the peak pressure of the beam was about 10^{-3} Torr in the scattering plane, as already mentioned. Thus, dependent on the angle of scattering, 20 to 50% of the scattered intensity were due to the background. This angular-dependent fraction was determined by a measurement in which the gas beam was switched off, but the same amount of gas was brought into the vacuum system by a separate inlet to generate an identical background pressure.

2.3. Scattering geometry

The scattering geometry is shown in figure 2. The gas beam is directed upwards, perpendicular to the scattering plane. The overlap volume of electron and gas beams is, as can be seen, independent of the position of the gun, and so of the angle of scattering.

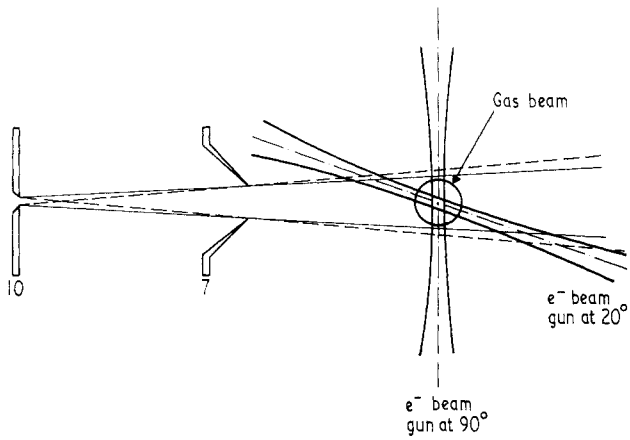

Figure 2. Scattering geometry. The electron beam is shown for 2 positions of the gun.

The apertures 7 and 10 define the angle of view of the detector. Their width and also the diameter of the gas beam is enlarged in comparison to the distance between the apertures to show the essential aspects more clearly. As long as the gas beam is completely within the region defined by the two solid lines connecting the edges of the apertures 7 and 10, all electrons scattered from the beam will be detected with equal probability. This, together with the constant overlap volume of gas and electron beam, enables our apparatus to measure angular distributions directly without any instrumental falsification.

The conventional technique does not use a target gas beam but a scattering chamber, which may be the whole vacuum vessel. The difference between that approach and our

own may also be seen from figure 2 by just neglecting the gas beam and considering that the target gas density is constant all over the scattering plane. Then the scattering volume is only defined by the electron beam and the reception cone of the detector. This volume changes with angle, which is also the reason for the change of the background scattering intensity in our experiment mentioned some paragraphs above.

To correct for this change is not easy. Assuming a thin and parallel electron beam, the variation of the scattering volume is roughly given by the reciprocal value of the sine of the scattering angle, but unfortunately the spread of the beam is normally not negligible. In the latter case, good knowledge of the intensity distribution in the electron beam and its variation along the beam path is necessary to compute the scattering volume with sufficient accuracy, but such knowledge has not been reported up to now in low-energy electron scattering work. In fact, it is not trivial to measure the intensity distribution of an electron beam of only a few electron volts of energy.

2.4. Adjustment problems and sources of systematic error

The advantage of the crossed beam technique is that no knowledge about the intensity distribution of the electron beam is required, provided the overlap of both beams does not change during the measurement. To make sure of this was our main problem in the present experiment. In our device the scattering angle is, as mentioned already, varied by rotating the gun and not the detector. If the centre of rotation of the gun does not coincide with the axis of the target gas beam, there will be a systematic variation of the overlap of the beams when the gun is moved. It was found that a deviation of 0·1 mm from the ideal adjustment was sufficient to change the scattered intensity by about 5%. Unfortunately a more precise fitting of the gas inlet system was not possible, but the problem was solved by fastening it to the gun, so that the relative position of both remained unchanged when the gun was swept.

It may be thought that in this way we only transferred the adjustment problem from the gun to the detector, but this is not the case. As can be seen from figure 2, the angle of view of the detector is slightly wider than the least angle necessary to see the whole gas beam (in our case 2·6 mm compared with 2 mm width of the gas beam). So, if the distance between the centre of the gas beam and the axis of rotation is not more than 0·3 mm, the gas beam, as seen from the detector, of course moves when the gun is swept, but does not leave the angle of view, and the probability of detection does not vary.

There remains one problem, and this is caused by the residual magnetic field. We compensated the earth's magnetic field (about 350 mG in our country) by two pairs of Helmholtz coils, and additionally used Mumetal shielding. Unfortunately, the latter was not in the best condition, and there remained a vertical magnetic field component of about 2 mG and a horizontal component of about 6 mG which pointed roughly in the forward scattering direction. When the gun, and with it the electron beam, is swept in such a field, the inhomogeneities of the vertical component will deflect the beam to the right or to the left, whereas the horizontal component will move it up or down. We shall see later that the latter effect is negligible, but the former is very dangerous as it causes a change of the overlap of electron and gas beams. There may be a systematic error of some per cent in our data due to this deflection in the magnetic field. It should be mentioned here that our apparatus originally was constructed for high-energy resolution studies of fine structures in the differential cross section (Andrick *et al* 1968), and not for angular distribution work. In the former work it was an advantage that the detector was in a fixed position. On the contrary, in an apparatus constructed for the measurement

of angular distributions it is safer to adjust for the different scattering angles by sweeping the detector and not the gun. This should be considered in future experiments.

2.5. Detector

For correct performance of the apparatus it is of course not only necessary that all electrons scattered from the gas beam have equal chances of passing aperture 10 (see figure 2), but also that any electrons doing this have equal chances of being counted. Because of the earlier work mentioned above, our apparatus is equipped with energy analysers in the detector also. These would in principle not have been necessary in the present experiment, as the energy selection in the gun was sufficient. Moreover, we could not make use of their selecting power as this might have caused different detection probabilities for electrons that passed aperture 10. To avoid this, the output apertures and the input aperture of the second analyser were widened so much that any electron of the energy distribution generated by the gun could traverse both selectors. Thus there was no disadvantage in leaving the analysers in place; on the contrary even with reduced selecting power, they were of use in reducing the background of slow electrons caused by scattering of the primary electron beam from the surfaces of the apparatus. In contrast to the gun, the analysers in the detector were tuned for a transmission energy equal to the energy in the collision region. This was done to keep the path from the scattering centre to the entrance aperature 10 free of electrostatic fields which would produce lens effects and deflect the electrons. The absence of such fields was always assumed in § 2.3. To check the detection probability for the scattered electrons, a thin metal pin of about 0·2 mm diameter, pointing perpendicular to the plane of figure 2, was moved through the scattering centre across the angle of view of the detector. If the electron gun was swept to a scattering angle of 90°, the pin remained on the axis of the electron beam during its motion. This could be controlled by measuring the current being absorbed by the pin, which was insulated for this purpose. The current observed was independent of the position of the pin, if the electron beam was well adjusted. Then also the number of electrons scattered from the pin was constant, and counting these as a function of the position of the pin gave the reception profile of the detector. An example of such a measurement is given in figure 3. The trapezoidal shape is expected from the

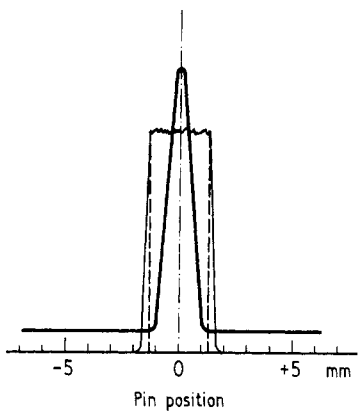

Figure 3. Acceptance profile of the detector in comparison with the density distribution of the target gas beam.

fact that the diameter of the second aperture limiting the scattered beam is smaller than that of the first aperture. Thus from a certain part of the electron beam path (and the target gas beam) the second aperture is fully seen through the first one. The length of this plateau is, of course, the one computed from the diameters and distances of the apertures 7 and 10. For comparison, the gas beam shape is also given and it can be seen that it is in fact well inside the region of constant detection probability.

To be honest it must be said that the profile was not always as good as shown in figure 3. It has not been mentioned yet that the apertures 7 and 10 are not slits, but circular holes. If the electron beam does not cross the axis of these both apertures, but runs slightly higher or lower, the width of the plateau in the detection profile will be reduced. The same will happen if the diameter of the electron beam is not small compared with the diameter of aperture 7. For future work we would recommend the use of vertical slit for aperture 7. One might also consider removing this aperture completely, as the angular resolution of the apparatus is anyway determined by the width of the gas beam and of aperature 10 only (in our case about 1·2 degrees). In fact, the role of aperture 7 is only to reduce the background scattering signal by limiting that part of the electron beam path from which electrons can be scattered through aperture 10. If, for example, in an apparatus pumped differentially, the target density is sufficiently low outside the beam, one may be able to do without such an aperture.

2.6. Energy calibration

The energy of the electrons is the sum of the transmission energy of the selector, the accelerating or decelerating voltage applied between aperture 3 and the collision region, and contact potentials between the different materials from which the electrodes may be machined. Even if all parts close to the electron beam are made from the same material there may be different surface potentials from different contamination; additionally there may be layers of high resistance on some apertures which, if hit by the electron beam, will charge up. All these effects make a determination of the collision energy unreliable, so that it is preferable to calibrate the apparatus by measuring a structure in the cross section the energetic position of which is known. We took the well-known ^2S resonance in helium and assumed the energetic position of this state to be 19·31 eV (eg Kuyatt 1968). More recent measurements indicate a slightly higher value (Sanche and Schulz 1972, Cvejanović *et al* 1974), which shifts our energy scale by about 60 meV. As the differential cross section, apart from resonance structures, varies slowly with energy, this shift will not be of importance for our results.

2.7. Measurement of the angular distribution

After adjustment of the electron beam and detector, a check of the detection profile as described above, and a check of the symmetry of the scattered signal by measuring at some angles on both sides of the forward direction, the angular distributions were measured in the following way.

Starting from the outermost scattering angle, ie 145° on the one or 100° on the other side, the scattered electrons were counted in angular steps of 5 or 10°. The counting time at any scattering angle was 6 seconds, during which some thousand to ten thousand counts were recorded. No measurement was made at 5° (and of course 0°), as the background from the unscattered electron beam rises rapidly below 10°. The value at 10° was often unreliable also. Having traversed the whole angular range on both sides of

the zero direction, the gas beam was switched off, and the whole procedure was repeated with background target gas to find the part of the scattered intensity not due to the beam (see § 2.2). The pressure in the apparatus was recorded continuously. Slight variations of about 1 % were observed during a run, which took about half an hour.

Finally, the measurements at 90° were repeated once more to check the stability of the apparatus. The counting rates, ie the angular distribution in arbitrary units, both for the measurement with and without gas beam were fed to a computer program, together with the pressure variation during the run. The latter could be described by a linear function. The program supplied any counting rate N with its statistical error $\sqrt{N}$, corrected for the pressure variation, and averaged the data obtained on both sides of the zero direction. An error was assigned to the result according to the Gaussian law of propagation, and these data were punched on cards for further processing using the programs described in the following section.

We have restricted our investigation to the energy interval from 2 to 19 eV. The lower bound is an experimental one, as we were not sure of sufficient focusing of our electron beam and equal transmission properties of our detector for all scattered electrons at smaller energies. The upper limit is set by the intended phase shift analysis which is—at least in principle—only possible as long as the scattering is purely elastic.

The measurements were not made one after another without interruption, but in four different series, between which the apparatus was partly or completely readjusted. On one occasion the gas beam source was removed and built in again, as the apparatus was used for a different experiment between two series. In addition, the 'electrical adjustment' ie the optimal selection of the voltages applied to the different electrodes and apertures, was remade for every angular distribution. For this reason we believe that there are no systematic errors common to all measurements, but that these errors, which are doubtlessly present in the single distributions (see §§ 2.4 and 4.2), are changed in each case.

3. Evaluation

To enable a detailed comparison with theory, but also to check the experimental results, the measured angular distributions were analysed for the elastic phase shifts. Moreover, it is possible to bring a relative measurement to an absolute scale by phase shift determination.

3.1. Theoretical background

If spin does not play a role in the scattering process, the differential elastic cross section is given by (eg Mott and Massey 1967)

$$\frac{\mathrm{d}\sigma}{\mathrm{d}\Omega} = |f(\theta)|^2 \tag{1}$$

$$f(\theta) = \frac{1}{2\mathrm{i}k} \sum_{l=0}^{\infty} (2l+1)[\exp(2\mathrm{i}\eta_l) - 1] P_l(\cos\theta) \tag{2}$$

where f is the scattering amplitude and P_l are the Legendre polynomials. k is the wave number of the free electron. The scattering phase shifts η_l are real for pure elastic scattering. In low-energy electron–rare gas atom scattering the first few partial waves

dominate. The higher partial waves must not be neglected completely, but should be considered in a simple approximation (eg Thompson 1966). Roughly speaking, they do not penetrate the inner part of the atom and so only feel the longest range part of the electron–atom interaction. This is the dipole polarization potential. As long as the phase shifts remain small they may be computed in Born's approximation with sufficient accuracy. This leads to the expression

$$2ikf(\theta) = \sum_{l=0}^{L} (2l+1)[\exp(2i\eta_l)-1]P_l(\cos\theta)+C_L(\theta) \tag{3}$$

with

$$C_L(\theta) = 2i\pi\alpha k^2\left[\tfrac{1}{3}-\tfrac{1}{2}\sin\frac{\theta}{2}-\sum_{l=1}^{L}\frac{1}{(2l+3)(2l-1)}P_l(\cos\theta)\right] \tag{4}$$

(eg Thompson 1966). α is the atomic polarizability which is 1·39 au in the case of helium. For this target $L = 2$ is sufficient anyway, and we shall see later that even the d-wave ($l = 2$) is in good agreement with Born's approximation.

It is often argued that, in principle, the determination of phase shifts from the differential cross section needs absolute values of the latter. Of course, the expression

$$a_l P_l(\cos\theta)$$

which is the general form of the right-hand side of equation (2) may be brought to any magnitude with conservation of its shape by multiplication of all a_l by the same factor. This means that if the a_l were arbitrary complex numbers, only their ratios could be determined but not their absolute magnitudes. In fact, the a_l are not arbitrary numbers, but special nonlinear functions of the phase shifts η_l, and the latter are real in the energy range below all inelastic thresholds. So the question becomes whether it is possible to find an alternative set of real numbers η_l' so that

$$\exp(2i\eta_l)-1 = A[\exp(2i\eta_l')-1] \tag{5}$$

with equal complex A for all l. Apart from some special cases, this is not possible if more than one partial wave takes part in the scattering. One may say that it is the interference among the partial waves which allows for the unique determination of the phase shifts from relative data. The more interference that takes place, the higher is the accuracy to be expected in the derived phase shifts.

3.2. *Method of phase shift analysis*

The phase shifts are found from the measured distribution by a fitting procedure. $d\sigma/d\Omega$ is calculated from equations (1), (3) and (4) with a trial set of phase shifts and is compared with the experimental data. The quality of the trial set is measured by

$$\chi^2 = \frac{1}{N-P}\sum_{i=1}^{N}\left(\frac{X_i-x_i}{\Delta X_i}\right)^2. \tag{6}$$

Here the X_i are the experimental points, which are assigned with errors ΔX_i. Their number is N. The x_i are the corresponding values computed from the trial set. P is the number of fitted parameters.

χ^2 is expected to be unity if the trial set agrees with the exact parameters and if the errors ΔX_i are the statistical ones. If no trial set can be found which brings χ^2 close to unity, the expression used to fit the experimental data is not suitable. The reason may

be that there is an unknown systematic error in the experiment, which cannot be reproduced by the expression. Computer fits to differential cross sections of low-energy electron scattering have been done several times (Hoeper *et al* 1968, Bransden and McDowell 1969, McDowell 1971). To find the best set of phase shifts, ie the one giving the lowest χ^2, so-called trial and error procedures or gradient search techniques were used. Starting from a parameter set estimated to be reasonable these programs look for the direction in the parameter space in which χ^2 is most reduced and choose a more refined set in this direction. Thus, following the gradient of the error hypersurfaces, the programs continue until they are stopped at a minimum. One disadvantage of these procedures is that they may be trapped in a local minimum, another that they only provide the best fit and no information on sets of the parameters which might also yield an almost as good result within the statistical error limits.

We have therefore used a different approach which is possible if the number of parameters to be fitted is small. All parameters were varied independently in their range of interest with a suitable step-width, and χ^2 was computed for any of their combinations. In cases where more than three data points diverged by more than 5% from the value calculated from the phase shift combination this combination was ruled out. The maximum and the minimum values of the phase shifts occurring in the remaining combinations were displayed, together with the values giving the lowest χ^2. Thus we could assign errors to our best fit data. As we have statistical errors of 0·5 to 1·5%, the allowed divergence of 5%, together with the possibility that this limit may be exceeded at three data points, means that we take account of systematic errors up to about 3 to 4%. This seems to be appropriate considering the experimental situation discussed in § 2.4. We shall see in § 4.2.2 that we rather overestimate the systematic errors this way.

For the comparison of measured and computed data, first the experimental result has to be brought to a suitable scale, as our apparatus does not allow the determination of absolute differential cross sections. The scale may be set by equating the values at one scattering angle. Often 90° is chosen, or a maximum of the intensity, but also other angles are used if they yield a better optical impression. The disadvantage is that only one, or in the best case a few data points, are used for the calibration, and that there is an arbitrariness in the choice of the normalization point. So we have preferred to use the total cross section ie to multiply the measured data by a factor F, so that the total cross section computed from them becomes equal to the total cross section $\sigma_0(\eta_0, \eta_1, \eta_2)$ belonging to the phase shift combination under trial:

$$\sigma_0(\eta_0, \eta_1, \eta_2) = \int \frac{d\sigma}{d\Omega} d\Omega \tag{7a}$$

$$\int \frac{d\sigma}{d\Omega} d\Omega = 2\pi \int_0^\pi \frac{d\sigma}{d\Omega} \sin\theta \, d\theta \tag{7b}$$

$$2\pi \int_0^\pi \frac{d\sigma}{d\Omega} \sin\theta \, d\theta \approx 2\pi \sum_{i=1}^{N} \left(\frac{d\sigma}{d\Omega}\right)_i \sin\theta_i \frac{\pi}{N} \tag{7c}$$

$$2\pi \sum_{i=1}^{N} \left(\frac{d\sigma}{d\Omega}\right)_i \sin\theta_i \frac{\pi}{N} = F \frac{2\pi^2}{N} \sum_{i=1}^{N} S_i \sin\theta_i. \tag{7d}$$

Here the S_i are the experimental data obtained at the scattering angles θ_i. The latter are equally spaced ranging from 0 to π. In our case where the measurement was made in angular steps of 5 degrees we have $N = 36$.

The computation of the right-hand side of equation (7*d*) requires an extrapolation of the measured distribution to the unmeasured range below 15 and above 145 degrees. Fortunately, the contribution of these ranges is strongly reduced by the weight $\sin\theta$ which has the property of being the lower as the more doubtful the extrapolation becomes approaching the end of the interval. Comparison of the initial extrapolation and the final best fit showed that the error in the factor F was lower than 1 %. It is to be noted that in this way an experiment can be brought to an absolute scale which originally yields relative data only. This means that the shape of the angular distribution determines the absolute value of the total cross section. The procedure is applicable successfully only under suitable circumstances, namely if the number of phase shifts to be considered is not too large. Also the statistical scatter of the data points and their angular spacing must not be too high so that the shape of the distribution can be identified unambiguously. So it seems that the method presently is only applicable to elastic scattering on rare gas atoms below the first inelastic threshold, and it is doubtful already if it will work with the heavier ones such as krypton and xenon.

4. Results and discussion

4.1. Angular distributions

Four of the 35 angular distributions measured altogether are given in table 1 and figure 4. The data have been normalized according to § 3.2. The shape of the distribution changes from pronounced backward scattering at low energies via a minimum around 70° at about 8 eV to predominantly forward scattering at the highest energies measured. This development can easily be understood from the general behaviour of the s- and p-wave phase shift as a function of the energy (eg Andrick 1973). Comparison is made with the work of Ramsauer and Kollath (1932) and Gibson and Dolder (1969a). The poor angular resolution of the apparatus of Ramsauer and Kollath leads to a flattening of the angular distributions, additionally there is a too steep rise towards small scattering angles which shows that the $\sin\theta$ correction is not sufficient (see § 2.3). This rise to small angles occurs often in scattering chamber experiments. The background scattering rate in our own experiment shows the same behaviour. Considering both these sources of error in the experiment of Ramsauer and Kollath the discrepancies between their results and ours can be explained.

The deviation of the data of Gibson and Dolder (1969a) is more complicated. Mistrusting the $\sin\theta$ correction, these authors calibrated their apparatus by an angular distribution computed from phase shifts which were deduced from the shape and magnitude of the helium resonance at 19·3 eV (Gibson and Dolder 1969b). Errors in these phase shifts lead to distortions of the correction function and to corrected data, the behaviour of which cannot be discussed in terms of instrumental effects. An additional question is if a correction found at 19 eV can be transferred to other energies in cases where the $\sin\theta$ correction fails, as the reason for the failure of this correction is that the finite diameter and divergence angle of the electron beam play a role, both quantities which normally are not kept constant with energy.

4.2. Phase shift analysis

4.2.1. Single energy fits. Each of the 35 measured angular distributions was analysed for phase shifts separately. The method outlined in § 3.2 was used, and in a first step the

Table 1. Examples of measured angular distributions. Column A, differential cross section (in $Å^2\,sr^{-1}$); column B, statistical error of the values in column A in parts per thousand.

	2 eV		5 eV		12 eV		19 eV	
θ	A	B	A	B	A	B	A	B
15	0·230	29	0·250	13	0·460	12	0·561	7
20	0·255	23	0·257	11	0·415	12	0·509	6
25	0·272	21	0·264	10	0·393	11	0·455	6
30	0·282	19	0·267	10	0·360	11	0·410	6
35	0·290	18	0·268	9	0·339	11	0·363	6
40	0·299	17	0·277	9	0·319	11	0·336	6
45	0·322	16	0·285	8	0·305	10	0·302	7
50	0·335	15	0·294	8	0·287	11	0·277	7
55	0·357	14	0·311	9	0·279	11	0·258	7
60	0·377	14	0·321	8	0·273	11	0·237	7
65	0·394	13	0·340	7	0·274	11	0·226	7
70	0·410	13	0·355	7	0·270	10	0·215	8
75	0·437	12	0·374	7	0·272	10	0·209	8
80	0·470	12	0·387	7	0·275	10	0·206	8
85	0·489	11	0·403	7	0·271	10	0·203	8
90	0·511	11	0·425	6	0·281	10	0·199	8
95	0·534	11	0·446	6	0·294	10	0·204	8
100	0·541	11	0·470	6	0·297	10	0·201	8
105	0·557	15	0·498	8	0·313	14	0·211	11
110	0·591	15	0·512	8	0·322	14	0·212	11
115	0·601	15	0·536	8	0·327	14	0·213	11
120	0·616	15	0·581	8	0·347	13	0·217	11
125	0·618	15	0·587	8	0·350	14	0·222	11
130	0·648	15	0·607	8	0·366	14	0·225	11
135	0·647	16	0·635	8	0·387	13	0·233	11
140	0·672	15	0·657	8	0·388	14	0·243	11
145	0·687	16	0·665	8	0·405	14	0·244	11

s-, p- and d-wave phase shifts were varied. The result for the d-wave is given in figure 5 in comparison with Born's approximation. The good agreement is obvious, so that it is sufficient to take the Born value for the d-wave also, and to use only the s- and the p-phase as adjustable parameters. This has the advantage, apart from saving computer time, that the error hypersurface becomes a function of two variables only which can be presented in a lucid way. This is done in figure 6 for the measurement at 12 eV from figure 4 and table 1. χ^2 shows a clear minimum, which might be considered as the experimental proof for the statement in § 3.1 that the phase shifts can be deduced from the shape of the angular distribution only and that absolute values of the differential cross section are not required. Though a wrong value of one of the phase shifts cannot be compensated fully by the other one, a partial balance is possible, predominantly by moving along the main axis of the ellipses of equal χ^2. This axis rotates with the collision energy. It becomes $\eta_0 = constant$ between 7 and 8 eV and runs about perpendicular to its direction in figure 6 at 2 eV.

So far we have only considered the statistical errors. Apart from these, systematic errors are present (see § 2.4), as we can see from the fact that for most angular distributions the χ^2 of the best fit (labelled χ^2_A in table 2) is significantly greater than one, especially if the statistical errors are smaller than one per cent. To take account of the systematic

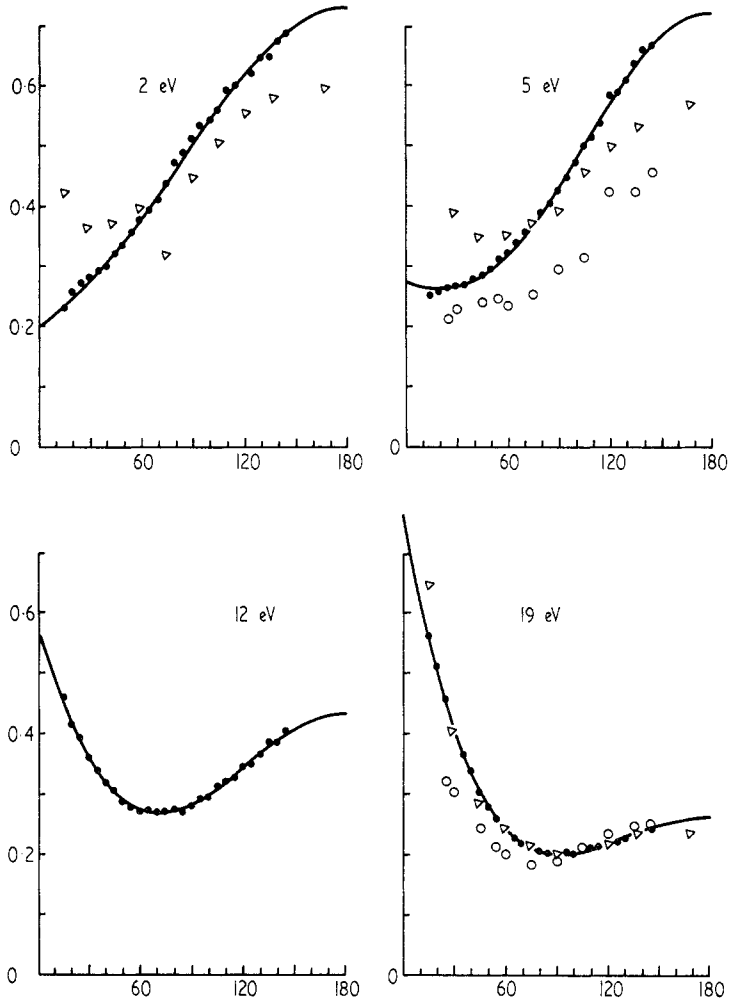

Figure 4. Differential cross section for e^-–He scattering. Vertical scale: $Å^2\ sr^{-1}$. Open triangles, Ramsauer and Kollath (1932) at 1·8, 5·35 and 19·2 eV respectively; circles, Gibson and Dolder (1969a) at 5·1 and 19·1 eV, respectively; full circles and full curve, this work.

errors, we have allowed for a deviation up to 5% from the measured shape in the fits (see § 3.2). This is also indicated in figure 6 by the broken line labelled '5%'; additionally the limits for 10% are marked. All phase shift combinations within this region we consider to be compatible with our measurement. We find the error limits for the phase shifts from the maximum and minimum values occurring in the combinations. The somewhat ragged shape of the limits is due to the fact that it is not always the same data point in the angular distribution which is the third one lying beyond the 5 or 10% boundary. The cusps indicate those points where a different value becomes responsible for exceeding the limits.

We believe that we tend to overestimate the errors of our phase shifts this way, but we do not currently feel justified in reducing the limits. Moreover, the error bars in figures 7 and 8 demonstrate the high accuracy (namely better than 5%) that has to be

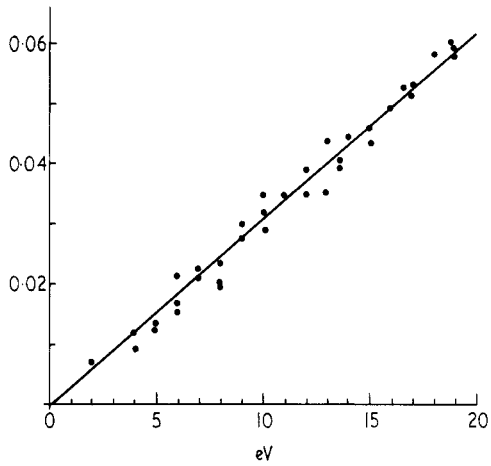

Figure 5. d-wave phase shift of e^-–He scattering against energy. Vertical scale: radians. Full circles, values from single energy fits; full line, Born's approximation.

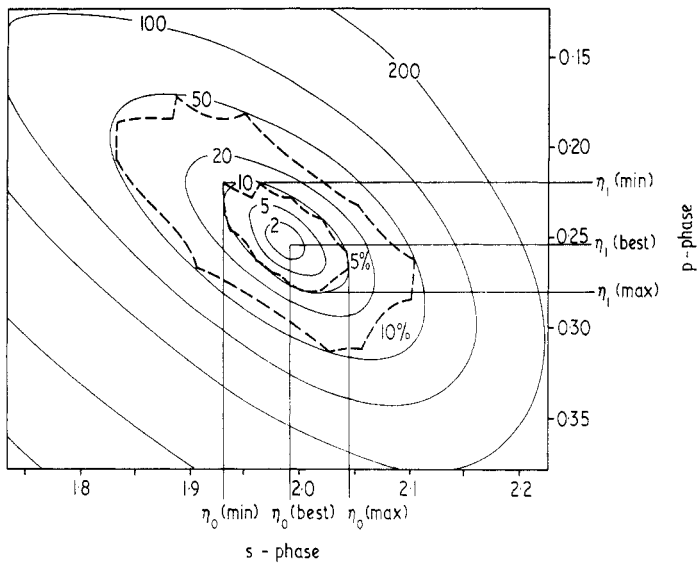

Figure 6. Error surface of s- and p-wave at 12 eV. The full contour lines refer to constant χ^2, the broken ones give the limits of agreement with the measurement to better than 5 and 10%.

achieved if one wants to decide which of the most advanced recent theoretical results is to be preferred.

4.2.2. Fitting to effective range formulae. If we assume that the systematic errors of the single distributions are independent, we can treat them as statistical errors in a least-squares fit through the phase shift values obtained in the single energy fits. We may use

Table 2. Examples of results of the evaluation (data from table 1). Column A, χ_A^2 and χ_B^2 (see text), phase shifts η_0 and η_1 in radians, total cross section σ_0 and momentum transfer cross section σ_m in Å^2; column B, error of the quantities in column A in per cent.

	2 eV		5 eV		12 eV		19 eV	
	A	B	A	B	A	B	A	B
χ_A^2	1·58		2·99		0·81		1·96	
χ_B^2	1·68		4·51		1·20		3·02	
η_0	2·616	5	2·323	2	1·985	3	1·814	5
η_1	0·052	37	0·135	19	0·259	12	0·325	12
σ_0	6·2	50	5·64	11	4·15	4	3·19	4
σ_m	7·2	40	6·64	11	4·28	3	2·86	4

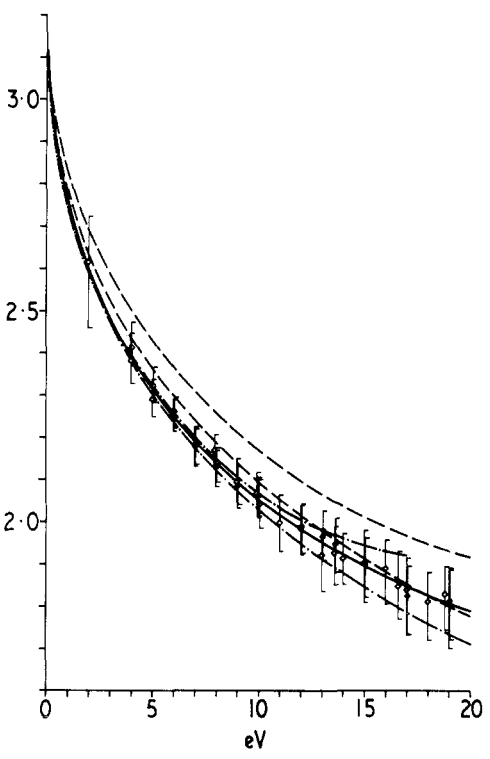

Figure 7. s-wave phase shift of e^-–He scattering against energy. Vertical scale: radians, zero suppressed. Broken curves (from top), Bransden and McDowell (1969), Callaway *et al* (1968); chain curves (from top), Burke *et al* (1969), Burke and Robb (1972); open squares and full curve, this work.

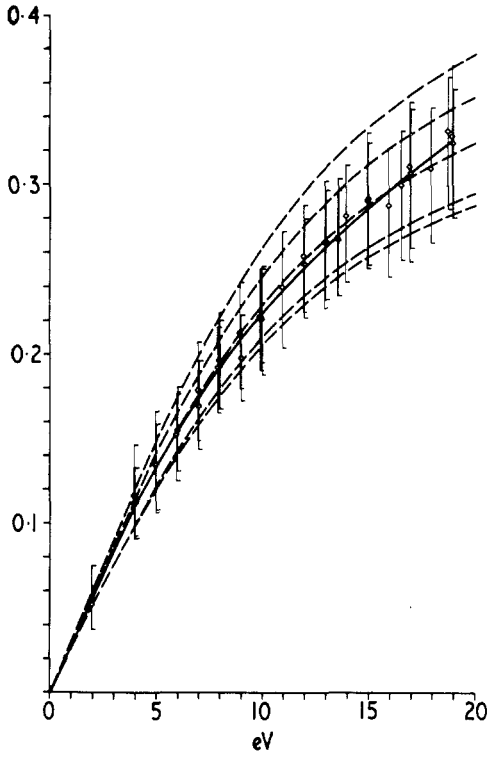

Figure 8. p-wave phase shift of e^-–He scattering against energy. Vertical scale: radians. Broken curves (from top), LaBahn and Callaway (1964), Duxler *et al* (1971, static exchange), Duxler *et al* (1971, polarized orbitals), Callaway *et al* (1968), LaBahn and Callaway (1966); open squares and full curve, this work.

the effective range formula (eg O'Malley *et al* 1961)

$$\cot \eta_0(k) = \frac{1}{a_0}\left[-\frac{1}{k}+\frac{\pi\alpha}{3}+\frac{2\alpha}{3}k\ln\left(\frac{\alpha k^2}{16}\right)\right]+\sum a_i k^i \tag{8}$$

for the s-wave and

$$\eta_1 = \sum a_i k^{2+i} \tag{9}$$

for the p-wave. Here α is the atomic polarizability, k is the wave number and a_0 in equation (8) is the scattering length. The a_i are treated as adjustable parameters. The result is given in figures 7 and 8. The χ^2 of these fits is 0·07 for the s-wave and 0·025 for the p-wave, thus indicating that the error bars may be reduced by about a factor of four and six respectively if there are no common systematic errors. We may also give the coefficients of the best fits. They are

$$a_0 = 1{\cdot}172 \qquad a_1 = 1{\cdot}939 \qquad a_2 = -0{\cdot}781$$

for the s-wave and

$$a_0 = 0{\cdot}308 \qquad a_1 = 0{\cdot}473 \qquad a_2 = -0{\cdot}824 \qquad a_3 = 0{\cdot}314$$

for the p-wave. Addition of further parameters did not reduce the χ^2 significantly, though it changed some of the parameters markedly. It should be emphasized that, in contradiction to our phase shifts, these sets of parameters are not unique. They are only given here to allow the exact reproduction of our results to the reader who is interested in this. In particular, our measurements are also compatible with other values of the scattering length, but more data points at lower energies would be required to determine it exactly. Finally we may ask how well our phase shifts averaged according to equations (7) and (8) agree with the original angular distributions. This can be indicated again by χ^2, which we now compute not with the phase shifts from the single energy fits but with the averaged phase shifts. We call this quantity χ^2_B, and its values are given in table 2. χ^2_B is always greater than χ^2_A, which again demonstrates the presence of systematic errors. The difference is in most cases smaller than a factor of two, which means, considering statistical errors of the order of 1 %, that the discrepancy between the measured angular distributions and those computed from the averaged phase shifts in most cases does not exceed a few per cent.

4.3. Comparison with theory

In figure 7 comparison is made with some representative theoretical data and with the result of the phase shift analysis of Bransden and McDowell (1969). The latter values are excluded even by our error limits. The reason is that the analysis of Bransden and McDowell is predominantly based on the experimental data of Gibson and Dolder (1969a), which we have discussed already. Moreover, the total cross section data of Golden and Bandel (1965) and the momentum transfer data of Frost and Phelps (1964) have been used. We shall come back to the problems of these measurements later. Additional work of McDowell (1971) comes slightly closer to our results, but does not remove the main discrepancy.

The result of Callaway *et al* (1968) is representative of the most refined polarized orbital calculations. The differences from the work of other authors (eg Duxler *et al* 1971) would hardly be visible in the scale of figure 7. The values are markedly higher than ours in the range from 4 to 12 eV. Though we cannot rule out these data from our error limits, the results of Burke *et al* (1969) or Burke and Robb (1972) fit our data better in that energy region. The latter is very close to the calculation of Sinfailam and Nesbet (1972), which for this reason is not plotted separately in figure 7. Above 12 eV the phase shift of Burke *et al* leaves our values and starts to climb to the resonance at

19·3 eV. This part is certainly erroneous, as the calculation gives much too high a value for the width of the resonance. The correct width of about 10 meV, which is well-established experimentally (eg Andrick 1973), will not yield a visible deviation from the background phase shift below about 18 eV.

Our p-wave results plotted in figure 8 agree best with the calculation of Duxler *et al* (1971). The deviation in the shape from our best fit must not be taken seriously considering the scatter of our data points. The other results are not all outside the error limits of the single energy fits, but we are fairly sure that they cannot be right.

4.4. Total and momentum transfer cross section

Finally, we may discuss what we can say from our measurements about quantities other than the differential cross section. Possessing the phase shifts, we can compute the total and the momentum transfer cross sections and compare these with direct measurements or other work. This is done in figure 9 for the total cross section. We can see that all direct measurements, apart from some irregular features at low energies, agree in the shape of the total cross section as function of the energy. This is not surprising, as the absolute calibration of the apparatus is the main problem in these experiments. Thus the results differ predominantly by a scaling factor. Our data follow the same trend.

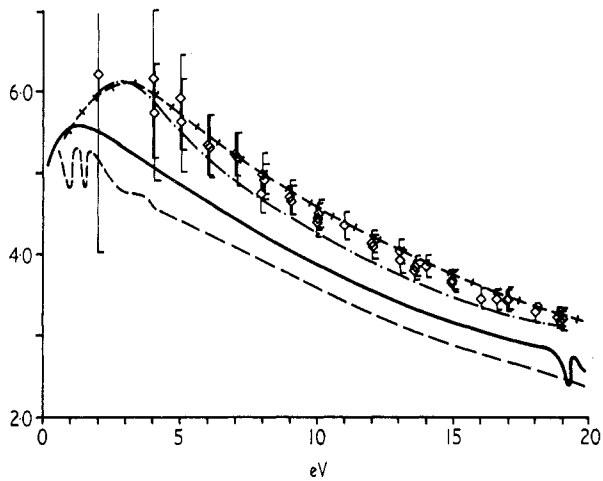

Figure 9. Total cross section of e^-–He scattering against energy. Vertical scale: $Å^2$, zero suppressed. Crosses, Ramsauer (1921); chain curve, Ramsauer and Kollath (1932); full curve, Golden and Bandel (1965); broken curve, Normand (1930); open squares, this work.

So we assume that our scaling factor is the right one as our result does not depend on absolute calibration of apparatus and it seems to be unlikely from our method that we can reproduce the shape but have the wrong scale.

The surprising result is that the total cross section predominantly referred to in the literature, namely the one of Golden and Bandel (1965), seems to be substantially wrong. It is about 10% lower than our data, though the authors state an error of only 3%. We find much better agreement with the work of Ramsauer (1921) and of Ramsauer and Kollath (1932). Our momentum transfer data are in agreement with Crompton *et al* (1970). Our error bars are obtained in the same way as those of the phase shifts, ie the

total and the momentum transfer cross section were computed for any phase shift combination giving not more than 5 % deviation from our measured angular distribution, and the maximum and the minimum of the occurring values were taken as upper and lower limits of the integral cross sections.

The much enhanced error bars at low energies are not due to inferior accuracy of the measurements, but predominantly to the fact that $\sin^2\eta_0$ and $\sin^2(\eta_0-\eta_1)$ with small η_1 respectively are the leading terms of the integral cross sections in this region so that the errors of η_0 are amplified considerably when the phase shift approaches π.

5. Summary

It has been shown that the long standing discrepancy between theory and experiment in low-energy electron–helium scattering can be removed, predominantly in favour of theory. Although there are systematic errors in our experiment, we are confident that we have obtained differential cross section data which have an accuracy better than 5 %. The data are consistent with basic theoretical principles (which cannot be said about all experimental results), and allow some of the recent theoretical findings to be ruled out.

Our method is expected to be limited to a few targets. Helium is very suitable, as only two phase shifts have to be determined to describe the differential cross section at low energies. It is to be hoped that, completing the information on this atom, theoretical methods can be improved and that the elastic scattering on helium can be used for instrumental calibration in the study of other targets.

References

Andrick D 1973 *Adv. Atom. Molec. Phys.* **9** 207–42
Andrick D, Ehrhardt H and Eyb M 1968 *Z. Phys.* **214** 388–401
Bederson B and Kieffer L J 1971 *Rev. Mod. Phys.* **43** 601–40
Bransden B H and McDowell M R C 1969 *Proc. Phys. Soc.* **2** 1187–201
Bullard E C and Massey H S W 1931 *Proc. R. Soc.* Ser A **133** 637–51
Burke P G, Cooper J W and Ormonde S 1969 *Phys. Rev.* **183** 245–64
Burke P G and Robb W D 1972 *J. Phys.* B: *Atom. Molec. Phys.* **5** 44–54
Callaway J, LaBahn R W, Poe R T and Duxler W M 1968 *Phys. Rev.* **168** 12–21
Chamberlain G E, Mielczarek S R and Kuyatt C E 1970 *Phys. Rev.* A **2** 1905–22
Crompton R W, Elford M T and Robertson A G 1970 *Aust. J. Phys.* **23** 667–81
Cvejanović S, Comer J and Read F H 1974 *J. Phys.* B: *Atom. Molec. Phys.* **7** 468–77
Duxler W M, Poe R T and LaBahn R W 1971 *Phys. Rev.* A **4** 1935–44
Frost L S and Phelps A V 1964 *Phys. Rev.* A **136** 1538–45
Gibson J R and Dolder K T 1969a *Proc. Phys. Soc.* **2** 1180–6
—— 1969b *Proc. Phys. Soc.* **2** 741–6
Golden D E and Bandel H W 1965 *Phys. Rev.* A **138** 14–21
Hoeper P S, Franzen W and Gupta R 1968 *Phys. Rev.* **168** 50–5
Kuyatt C E 1968 *Methods of Experimental Physics* eds B Bederson and W L Fite vol 7A (New York: Academic Press) pp 1–89
LaBahn R W and Callaway J 1964 *Phys. Rev.* A **135** 1539–46
—— 1966 *Phys. Rev.* **147** 28–40
McDowell M R C 1971 *Atomic Physics II* ed P G H Sandars (New York: Plenum) p 289
Massey H S W and Burhop E H S 1969 *Electronic and Ionic Impact Phenomena* vol I (London, New York: Oxford U P)
Mehr J 1967 *Z. Phys.* **198** 345–50
Mott N F and Massey H S W 1965 *The Theory of Atomic Collisions* 3rd edn (London, New York: Oxford U P)

Normand C E 1930 *Phys. Rev.* **35** 1217–25
O'Malley T F, Rosenberg L and Spruch L 1961 *Phys. Rev.* **125** 1300–10
Ramsauer C 1921 *Ann. Phys., Lpz.* **66** 546
Ramsauer C and Kollath R 1932 *Ann. Phys., Lpz.* **12** 529–61
Sanche L and Schulz G J 1972 *Phys. Rev.* A **5** 1672–83
Sinfailam A L and Nesbet R K 1972 *Phys. Rev.* A **6** 2118–25
Thompson D G 1966 *Proc. R. Soc.* Ser A **294** 160–74